Exploring the role of plant hydraulics in canopy fuel moisture content: insights from an experimental drought study on Pinus halepensis Mill. and Quercus ilex L.

Coffi Belmys Cakpo, Julien Ruffault, Jean-Luc Dupuy, François Pimont,
Claude Doussan, Myriam Moreno, Nathan Jean, Frederic Jean, Régis Burlett,
Sylvain Delzon, et al.

HAL Id: hal-04665786
https://hal.inrae.fr/hal-04665786v1

INRA@

Annals of Forest Science

Open Access

Exploring the role of plant hydraulics in canopy fuel moisture content: insights from an experimental drought study on *Pinus halepensis* Mill. and *Quercus ilex* L.

Coffi Belmys Cakpo[1,2†], Julien Ruffault[1*†], Jean-Luc Dupuy[1], François Pimont[1], Claude Doussan[3], Myriam Moreno[1], Nathan Jean[1], Frederic Jean[1], Regis Burlett[4], Sylvain Delzon[4], Santiago Trueba[4], José M. Torres-Ruiz[5,6], Hervé Cochard[5] and Nicolas Martin-StPaul[1]

Abstract

Key Message Understanding the impact of extreme drought on the canopy fuel moisture content (*CFMC*) is crucial to anticipate the effects of climate change on wildfires. Our study demonstrates that foliage mortality, caused by leaf embolism, can substantially diminish *CFMC* during drought on *Pinus halepensis* Mill. and *Quercus ilex* L. It emphasizes the importance of considering plant hydraulics to improve wildfire predictions.

Context Canopy fuel moisture content (*CFMC*), which represents the water-to-dry mass ratio in leaves and fine twigs within the canopy, is a major factor of fire danger across ecosystems worldwide. *CFMC* results from the fuel moisture content of living foliage (live fuel moisture content, *LFMC*) and dead foliage (dead fuel moisture content, *DFMC*) weighted by the proportion of foliage mortality in the canopy (a_{Dead}). Understanding how *LFMC*, a_{Dead}, and ultimately *CFMC* are affected during extreme drought is essential for effective wildfire planning.

Aims We aimed to understand how plant hydraulics affect *CFMC* for different levels of soil water deficit, examining its influence on both *LFMC* and a_{Dead}.

Methods We conducted a drought experiment on seedlings of two Mediterranean species: Aleppo pine (*Pinus halepensis* Mill.) and Holm oak (*Quercus ilex* L.). Throughout the drought experiment and after rewatering, we monitored *CFMC*, *LFMC*, and a_{Dead} along with other ecophysiological variables.

Results *LFMC* exhibited a significant decrease during drought, and as leaf water potentials reached low levels, a_{Dead} increased in both species, thereby reducing *CFMC*. Distinct water use strategies resulted in species-specific variations in dehydration dynamics.

Conclusion Our findings demonstrate that as drought conditions intensify, foliage mortality might become a critical physiological factor driving the decline in *CFMC*.

†Coffi Belmys Cakpo and Julien Ruffault contributed equally to this work.

*Correspondence:
Julien Ruffault
julien.ruffault@inrae.fr
Full list of author information is available at the end of the article

BMC

1 Introduction

The moisture content of vegetation, defined as the ratio of water to dry mass, is a major factor of fire danger across ecosystems worldwide (Finney et al. 2021). Live fuel moisture content (*LFMC*) refers to the moisture content of leaves and fine twigs in the canopy (Yebra et al. 2013), while dead fuel moisture content (*DFMC*) is the moisture content of fine dead material, such as litter (Matthews 2014). Recent evidence suggests that *LFMC* could play a substantial role in wildfires as it has been linked to increased burnt area (Nolan et al. 2016; Pimont et al. 2019a; Rao et al. 2022), the occurrence of extreme wildfire events (Ruffault et al. 2018a), and accelerated rates of spread in shrubland fires (Pimont et al. 2019b).

Predicting *LFMC* dynamics is a fundamental challenge in the face of climate change with increasing drought events (Ruffault et al. 2020; Torres-Ruiz et al. 2024), but our understanding of its spatial and temporal patterns remains limited. Several factors contribute to this uncertainty. First, *LFMC* is not only a function of weather conditions but also depends on species-specific traits, soil characteristic, and microclimate conditions that influence vegetation response to drought (Jolly and Johnson 2018; Nolan et al. 2020; Ruffault et al. 2023). Standard meteorological-based indices, including the drought code of the fire weather index (Van Wagner 1987), inadequately account for this complexity, resulting in limited predictive performance (Ruffault et al. 2018b). Furthermore, the definition of *LFMC* remains somewhat ambiguous. Some studies define *LFMC* at the leaf level, aligning with ground-based measurements (Martin-StPaul et al. 2018; Gabriel et al. 2021), while others define *LFMC* at the canopy level, integrating canopy heterogeneity and therefore matching with the scale of remote-sensing measurements (Yebra et al. 2013). To address this discrepancy, Ruffault et al. (2023) proposed differentiating *LFMC* as the fuel moisture content of individual leaves from the canopy fuel moisture content (*CFMC*) at the plant or canopy scale, a definition that is adopted in this study.

Plant desiccation under drought depends on a suite of plant and leaf anatomical and functional traits, ranging from characteristics of leaf cells to whole plant hydraulic architecture (Jolly and Johnson 2018; Nolan et al. 2020). Pressure–volume (*p–v*) curves (Tyree and Hammel 1972; Bartlett et al. 2012), which depict the relative water content of living cells as a function of leaf water potential (Ψ_{leaf}), have shown to offer a relevant framework to predict *LFMC* dynamics (Nolan et al. 2018; Pivovaroff et al. 2019; Scarff et al. 2021; Ruffault et al. 2023). According to this framework, the response of *LFMC* to Ψ_{leaf} is driven by several leaf traits, including the modulus of cell wall elasticity (ε, MPa), the osmotic water potential at full turgor (π_0, MPa), the leaf dry matter content (*LDMC*), and the fraction of symplasmic compartment in the leaves (α_f). By considering these leaf traits, it is possible to evaluate how *LFMC* dynamics may vary among species as Ψ_{leaf} decreases during drought (Nolan et al. 2020).

Accumulating evidence also shows that physiological processes related to plant hydraulic mechanisms should be taken into account for *CFMC* predictions (Ruthrof et al. 2016; Ruffault et al. 2023; Torres-Ruiz et al. 2024). Indeed, decreased plant water potentials induced by drought can lead to the cavitation of plant vessels and diminish *CFMC* either by decreasing the amount of water in organs affected by cavitation or by initiating foliage and branch mortality (Hölttä et al. 2009; Martin-StPaul et al. 2017). Hydraulic segmentation, which posits that leaves are more susceptible to drought-induced embolism than stems to protect vital perennial organs from irreversible hydraulic dysfunction (Pivovaroff et al. 2014; Johnson et al. 2016), is also a critical factor to consider to predict the rates of leaf mortality with increasing drought. However, the relative importance of these physiological mechanisms in *CFMC* dynamics has yet to be quantified, as well as the extent to which they might alter *CFMC* both during and after drought.

Four different hypotheses (summarized in Fig. 1) can be proposed to explain the physiological mechanisms underlying tree desiccation during extreme drought. The first hypothesis (H1) suggests that changes in CFMC are solely due to reversible variations in *LFMC* linked to the symplasmic water content (as explained by *p–v* curves). Conversely, assuming that hydraulic-induced damages are also involved in CFMC changes during drought, three alternative hypotheses can be made, depending on the scale at which hydraulic damages occur. If hydraulic damages occur at leaf scale only (H2), then apoplasmic leaf compartments are affected, and both *LFMC* and *CFMC* would not fully recover after drought. Alternatively, hydraulic failure could trigger foliage or branch mortality (H3), which means that the ratio of dead-to-live fuel (α_{Dead}) increases with decreasing Ψ_{leaf}, lowering the *CFMC*, but that *LFMC* fully recovers after rewatering. Last, a fourth hypothesis (H4) is that both mechanisms at

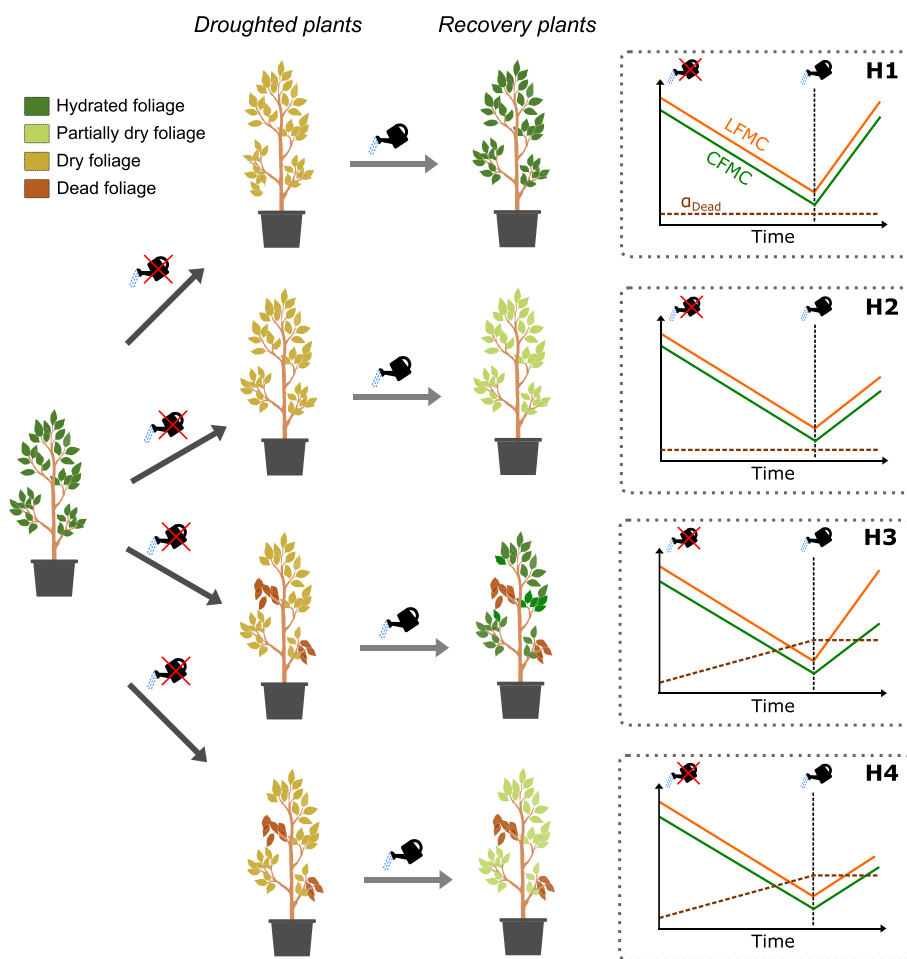Cakpo *et al. Annals of Forest Science*   (2024) 81:26

Page 3 of 16

Fig. 1 Schematic representation of the drought experiment and principal hypotheses (H) investigated in this study to understand the physiological mechanisms underlying seedings desiccation during and after drought. The figure depicts the theoretical dynamics of leaf-scale live fuel moisture content (*LFMC, orange lines*), plant-level canopy fuel moisture content (*CFMC, green lines*), and the proportion of dead foliage within the plant canopy (a_{Dead}, brown dashed line) for each hypothesis. H1: *LFMC* and *CFMC* fully recover to their initial levels after plant rewatering. H2: *LFMC* and *CFMC* exhibit incomplete recovery due to drought-induced leaf-scale damages. H3: *LFMC* recovers to its initial value, while *CFMC* remains incomplete due to drought-induced foliage mortality (increase in a_{Dead}). H4: *LFMC* and *CFMC* both exhibit incomplete recovery due to both drought-induced leaf-scale damages and foliage mortality (increase in a_{Dead})

the leaf and plant scales occur simultaneously, in proportions that remain to be quantified.

In this study, we investigated the impacts of a severe drought on the dynamics of *CFMC* and *LFMC* for two Mediterranean tree species (*Pinus halepensis* Mill. and *Quercus ilex* L.) both during and after (recovery) drought. We subjected seedlings of these two species to varying levels of severe drought-induced soil water deficits and assessed their recovery under each of these drought conditions. Then, *LFMC*, a_{Dead}, and *CFMC* for the seedlings were simulated based on Ψ_{leaf} using process-based models derived from *p–v* curves and vulnerability to xylem embolism. Specifically, we aimed to investigate (1) the predictability of *LFMC* using *p–v* curves; (2) the influence of

hydraulic damage on CFMC, including effects on leaf tissues and/or foliage and branch mortality; and (3) potential differences in *LFMC* and *CFMC* dynamics between the two species.

2 Material and methods

2.1 Plant material and experimental design

The experiment involved seedlings of two Mediterranean species: Aleppo pine (*Pinus halepensis* Mill.) and Holm oak (*Quercus ilex* L.). In February 2019, 84 2-year-old seedlings (42 per species) were carefully selected to ensure homogeneity in terms of size (height: 30 to 50 cm), crown volume, and foliage density. In early March 2019, the plants were transplanted into

Cakpo *et al. Annals of Forest Science*   (2024) 81:26

Page 4 of 16

2.5-l cylindrical plastic containers filled with organic soil comprising 50% topsoil, 32% peat, and 18% sand. From March 2019 to June 2019, plants were grown at the French National Forestry Office experimental forest nursery in Cadarache (lat.: 43.91°, long.: 4.87°; France). After this growth period, all potted plants were brought to the campus of INRAE at Avignon (lat.: 43.91°, long.: 4.87°; France) to start the experiment in the greenhouse facility of the campus. The experiment started on the 7th of July 2019 and ended on the 14th of September 2019. It was conducted in a greenhouse of type S2 comprising four compartments, each measuring 65 m². This greenhouse is equipped with two ventilated air temperature and relative humidity ventilated loggers (HD 9817T1) as well as two radiation loggers. The greenhouse temperature was maintained between 25 and 35 °C, the relative humidity (RH) was maintained between 40 and 75%, and the maximum diurnal photosynthetically active radiation (PAR) below 1000 μmol.m^{-2}.s^{-1}. All pots were saturated with water and covered with a plastic film to prevent soil evaporation.

Plants were subjected to various levels of water deficit and ecophysiological variables, and fuel moisture content was monitored during the drought period and after plant rewatering. Starting from full watering at the beginning of the experiment (day 0), and without further precipitation, six measurement campaigns were conducted at different time intervals (from day 0 to day 45) to cover a wide range of water potentials for each species (see measurement days in Appendix Table 3). On each sampling date (referred to as date D_d), a batch of six plants per species was selected to measure various ecophysiological variables (described below). At the end of each measurement day, the plants were randomly divided into two subsets of three plants each. One subset of three plants (referred to as *droughted plants*) was used for destructive estimation of moisture content (see below), while the other subset (referred to as *recovery plants*) was rehydrated to saturation to assess the recovery of physiological variables and moisture content. For the three recovery plants, the soil was maintained above field capacity, and additional measurements were conducted 2 days (D_{d+2}) and 6 days (D_{d+6}) after rehydration. Six days after rehydration, destructive estimations of moisture content were performed. A batch of six plants per species was used as a control treatment from the beginning of the experiment. For these plants, soil water was kept close to or above field capacity by watering the pots every 2 to 4 days. In addition to measuring live plants, we also examined the moisture content of litter to determine if the moisture levels of recently deceased leaves and litter exhibit similar patterns. Two batches of dead pine needles and oak leaves obtained from litter collected at a nearby mature forest with the same species (Moreno et al. 2021) were placed in the greenhouse at the start of the experiment to monitor the moisture content of the litter. The datasets acquired for this study are fully accessible in Ruffault and Martin-StPaul (2024).

2.2 Ecophysiological measurements

For each measurement campaign, water potentials and leaf gas exchanges were measured at D_d, D_{d+2}, and D_{d+6}. Plant transpiration was estimated at pot level through weightings. Water loss at the pot level was estimated through manual weight measurements, which were conducted twice daily using a FC6CCE-HX Sartorius balance: once in the morning at 8 am and once in the afternoon at 5 pm. For each campaign, leaf water potential was measured at predawn (Ψ_{predaw}) and at midday (Ψ_{midday}) for the targeted plants at D_d, D_{d+2}, and D_{d+6}. Samples were collected before sunrise (between 4 and 5 am) and between 1 and 3 pm for Ψ_{predaw} and Ψ_{midday} measurements, respectively. Water potential measurements were made using a Scholander pressure chamber (PMS model 1505 D) immediately after sample collection.

To examine the hypotheses linking foliage desiccation to cavitation levels, we compiled previously published data on vulnerability curves related to cavitation for the two species under study. For *Quercus ilex*, we gathered vulnerability curves for both leaves and stems. Stem measurements were obtained from Sergent et al. (2020) conducted on 1-m-long branches sampled from 10 individual trees using Cavitron techniques (Burlett et al. 2022). Vulnerability curves for *Quercus ilex* leaves were extracted from Moreno (2022) and were derived from samples collected at the Font-Blanche site using optical techniques. The Font-Blanche long-term experimental monitoring site is located in a mixed Mediterranean forest in South-Eastern France (43°14′27″N, 5°40′45″E; altitude 425 m above sea level). The site is dominated by *P. halepensis* in the upper tree stratum (average height, 13 m) and *Q. ilex* in the intermediate tree stratum (average height, 5 m). Vulnerability curves for *Pinus halepensis* were extracted from Moreno (2022), and these measurements were obtained using Cavitron techniques on 15 samples collected at the Font-Blanche site in 2018. Vulnerability curves were modelled according to the procedure described by Sergent et al. (2020).

2.3 Moisture content measurements

At the end of each measurement day (i.e., droughted plants at D_d and recovered plants at D_{d+6}), plants were designated for destructive measurements of moisture content. The aboveground parts of each plant were promptly divided into distinct compartments: young leaves, mature leaves, dead leaves, and wood. The

identification of dead leaves or needles was conducted by comparing their colors with those of the control plants. For pine trees, needles exhibiting a brown, yellow, or desiccated appearance were categorized as dead. However, for oak trees, only leaves displaying a brown or desiccated state were deemed dead. It is important to highlight that the distinction between live and dead leaves was more straightforward for oak trees due to their distinct brown coloration upon death. In contrast, the identification process for pine trees was more nuanced, as yellowing was also considered an indication of death. Each of these classes was weighed fresh and then put in the oven for 48 h at 60 °C to obtain the dry mass. The moisture content (FMC) of the plant and its organs (leaf and wood) were calculated on a dry mass basis such as the following:

$$FMC = 100\frac{F_W - D_W}{D_W} \qquad (1)$$

where F_W is the fresh weight (g) and D_W is the dry weight (g).

Furthermore, for each measurement campaign, three pots (50 cl) of dead pine needles and dead oak leaves were collected from litter batches to estimate the moisture content of dead fuels.

2.4 Soil water content

For each measurement campaign, the normalized soil water content (W_{norm}) was computed at D_d, D_{d+2}, and D_{d+6} for each pot using the following formula:

$$W_{norm} = \frac{W - W_r}{W_{Sat} - W_r} \qquad (2)$$

where W is the soil mass of the pot, W_r is the soil mass at residual water content, and W_{sat} is the water content at saturation. W_r was measured for each pot at the end of the experiment after drying the soil at 70 °C. W_{sat} was estimated at the beginning of the experiment, after the pots were irrigated at saturation. The mass of fresh trees was considered to be constant throughout the experiment.

2.5 Testing LFMC recovery after drought

To investigate whether *LFMC* fully recovered after drought (in accordance with H1 and H3; Fig. 1) or did not fully recover due to leaf-level hydraulic dysfunction

(in accordance with H2 and H4; Fig. 1), we examined the influence of the minimum water potential reached by the plant (Ψ_{min}) on LFMC recovery. For this purpose, among all recovered samples, we selected two groups for each species: rewatered leaves that were previously submitted to extreme drought (i.e., $\Psi_{min} < -4$ MPa for oaks and < -3.5 MPa for pines, respectively) and those that were not previously submitted to extreme drought ($\Psi_{min} > -3$ MPa for oaks and $\Psi_{min} > -2.5$ MPa for pines). These thresholds were adjusted empirically based on observed effects. We compared the LFMC of rewatered leaves in these two groups.

2.6 Model analysis

We developed a semiempirical modeling framework for estimating the canopy fuel moisture content (*CFMC*) based on the hypothesis developed in Fig. 1. Following Ruffault et al. (2023), *CFMC* can be computed as the weighted sum of live fuel moisture content (*LFMC*) and dead leaf fuel moisture content (*DFMC*) in foliage as follows:

$$CFMC = (1 - \alpha_{Dead})LFMC + \alpha_{Dead}DFMC \qquad (3)$$

where α_{Dead} is the mass proportion of dead foliage on a dry basis in the plant (foliage mortality).

LFMC is derived from Ψ_{Leaf} by p–v curves where it is a function of the moisture content in the symplasmic and the apoplasmic compartments weighted by their respective volumetric fractions such as the following:

$$LFMC = LFMC_{sat}\left[a_f RWC_{Apo} + (1 - a_f)RWC_{Sym}\right] \qquad (4)$$

where a_f is the fraction of the apoplasmic compartment in the shoots, $LFMC_{sat}$ (% dry mass) is the fine fuel moisture content at water saturation, RWC_{Apo} is the relative water content of the apoplasm, and RWC_{Sym} is the relative water content of the symplasm.

$LFMC_{sat}$ is determined as a function of leaf dry matter content (*LDMC*, the ratio of leaf dry mass to saturated fresh mass, $g.g^{-1}$) as in Ruffault et al. (2023):

$$LFMC_{sat} = \frac{1}{LDMC} - 1 \qquad (5)$$

RWC_{Sym} is calculated using the following equation depending on whether ψ_{Leaf} is below or above the turgor loss point (π_{TLP}, MPa) also derived from p–v curves (Bartlett et al. 2012):

$$RWC_{Sym} = \begin{cases} min\left(\dfrac{-(\psi_{Leaf} + \pi_0 - \varepsilon) \pm \sqrt{(\psi_{Leaf} + \pi_0 - \varepsilon)^2 - 4\varepsilon\psi_{Leaf}}}{2\varepsilon}\right), if\ \psi_{Leaf} > \pi_{TLP} \\[12pt] 1 - \left(1 - \dfrac{\pi_0}{\pi_{TLP}}\right), if\ \psi_{Leaf} \leq \pi_{TLP} \end{cases} \qquad (6)$$

Cakpo *et al. Annals of Forest Science*   (2024) 81:26

Page 6 of 16

where π_0 (MPa) is the osmotic potential at full turgor and ε (MPa) the modulus of elasticity of the symplasm.

According to hypotheses H2 and H4 (Fig. 1), leaf-scale hydraulic damages would cause a decline in apoplasmic leaf water content under drought such that RWC_{apo} could be variable over time. Preliminary results show that *LFMC* did not significantly differ between the plants that were or were not previously submitted to extreme drought (see Fig. 3 in results); this mechanism was not included in this model.

α_{dead} was modelled from an empirical sigmoidal function adjusted to the data as follows:

$$\alpha_{dead} = \frac{100}{1 + e^{\left(\frac{slope}{25}(\Psi_{min} - \Psi f_{50})\right)}} \tag{7}$$

where Ψ_{min} (MPa) is the minimum water potential reached by the plant (for a recovery plant, this is equal to Ψ_{midday} before rewatering).*slope* is the linear slope at the inflection point, and Ψf_{50} (MPa) is the water potential causing 50% foliage mortality.

DFMC is modelled according to Resco de Dios et al. (2015) as follows:

$$DFMC = FM_0 + FM_1 e^{-mVPD} \tag{8}$$

where FM_0 is the minimum *DFMC*, $FM_0 + FM_1$ the maximum *DFMC*, and m (%.kPa^{-1}) is an exponent parameter setting the rate of moisture decay with increasing VPD.

2.7 Fitting model parameters

The submodels (*LFMC*, α_{dead}, and *DFMC*) were parametrized using a genetic algorithm implemented in the GA (genetic algorithm) package (Scrucca 2013) within the R programming language (R Core Team 2023). For *LFMC*, three types of procedures were tested. First, the equations were fitted by optimizing the target parameters, namely π_0, ε, LDMC, and α_f. In this initial procedure, α_f was allowed to vary between 0.2 and 0.4 for both species, according to the range of values expected for this trait. In the second approach, α_f was held constant at 0, completely disregarding the apoplasmic compartment. The third approach involved allowing α_f to be determined freely by the fitting algorithm. The performance of the models was assessed by evaluating them against the data using several metrics, including the

root-mean-squared error (*RMSE*), mean absolute error (*MAE*), and coefficient of determination (R^2).

3 Results

3.1 Dynamics of plant dehydration

In both species, we observed a rapid and consistent drying of the plants submitted to soil water deficits throughout the experiment, with a decrease in normalized soil water content (W_{norm}), canopy fuel moisture content (*CFMC*), live fuel moisture content (*LFMC*), midday leaf water potential (Ψ_{midday}), and an increase in foliage mortality (α_{Dead}) (Fig. 2). Appendix Fig. 5 provides additional information on the dynamics of predawn water potential (Ψ_{pd}) and plant-level transpiration, showing consistent patterns with the observations of Ψ_{midday}. On the other hand, the dead fuel moisture content (*DFMC*) remained relatively stable (with some variability) throughout the experiment for litter samples and dead leaves and needles (Fig. 2E, F).

Differences in the dynamics of fuel moisture content were observed between the two studied species with pine consistently maintaining higher levels of *CFMC* and *LMFC* compared to oak (Fig. 2 A, B, C, D). Specifically, *LFMC* decreased from 176 to 64% and *CFMC* from 152 to 53% in pine during the experiment (Fig. 2B, D). In contrast, oaks exhibited a decrease in *LFMC* from 90 to 43% and a decrease in CFMC from 90 to 27% (Fig. 2A, C).

The dehydration dynamics also exhibited differences between the two studied species. Unlike oaks, which showed a decrease in *LFMC* and *CFMC* starting after the second measurement date, pines exhibited a steady decline in water content (*LFMC* and *CFMC*) during soil drying. Species-specific variations were also observed in the dynamics of Ψ_{midday} and α_{dead}. Measurements of Ψ_{midday} revealed a relatively consistent decline, with oaks reaching lower values (approximately -8.5 MPa) compared to pines (approximately -7 MPa). Throughout most of the experiment duration, α_{Dead} maintained its minimum value (14% for pines and 1% for oaks). However, a significant increase was observed when Ψ_{midday} dropped below -6 MPa in both species.

Recovery patterns varied across the variables studied and the level of drought reached by the droughted plants. Thus, W_{norm}, *LFMC*, Ψ_{midday}, and $\Psi_{predawn}$

(See figure on next page.)

Fig. 2 Dynamics of plant dehydration during drought and rewatering in oak (*Quercus ilex*) and pine (*Pinus halepensis*). The time dynamics of canopy fuel moisture content (*CFMC*, % dry mass) (**A**, **B**), live fuel moisture content (*LMFC*, % dry mass) (**C**, **D**), dead fuel moisture content (*DFMC*, % dry mass) (**E**, **F**), proportion of dead foliage (α_{dead}, %) (**G**, **H**), midday leaf water potentials (Ψ_{midday}, MPa), and normalized soil water content (W_{norm}) (K, L) are shown. The median of measured values, along with the 5th and 95th percentiles, are shown. Red and blue circles indicate the droughted and recovery pots, respectively, while black circles represent the litter
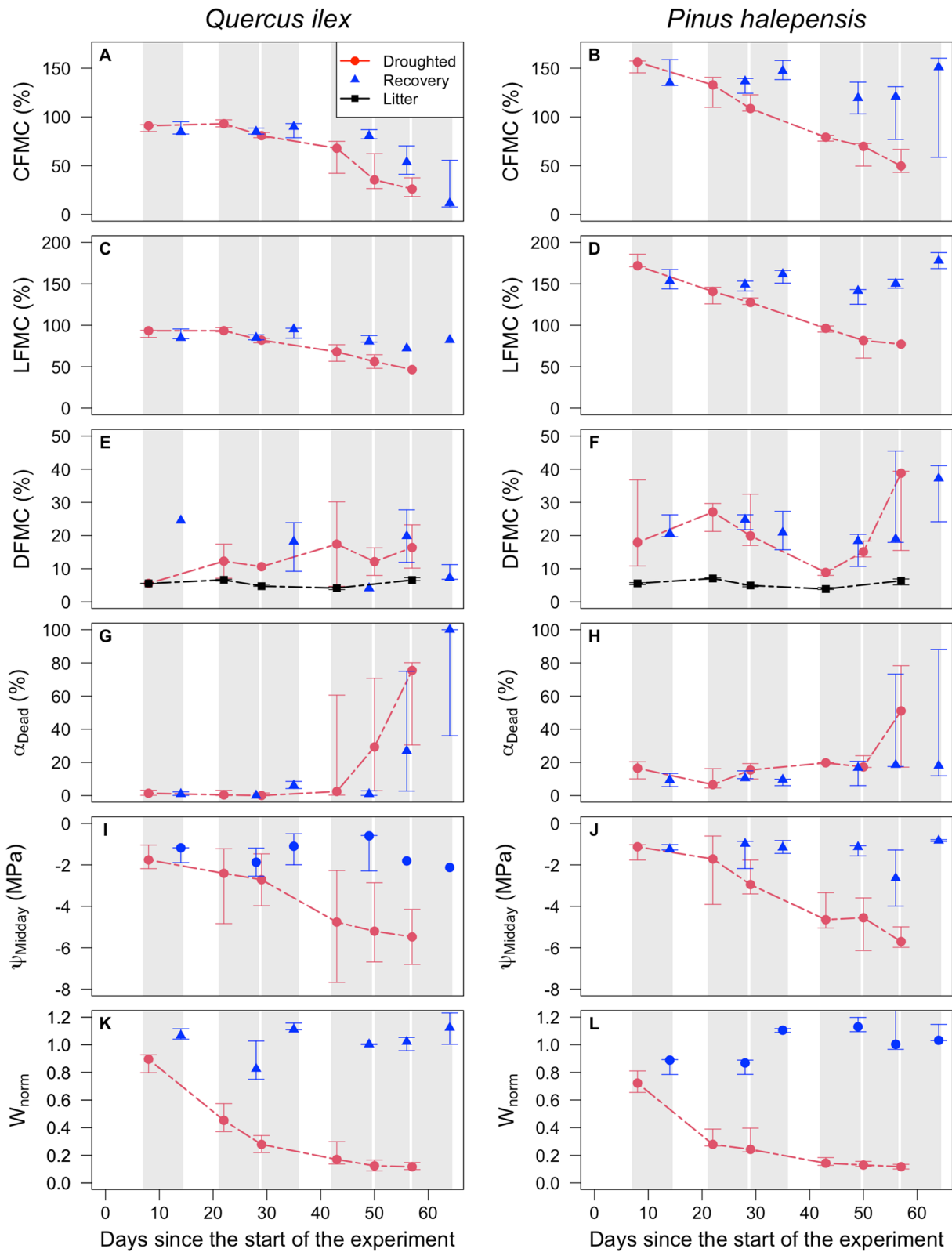
Fig. 2 (See legend on previous page.)

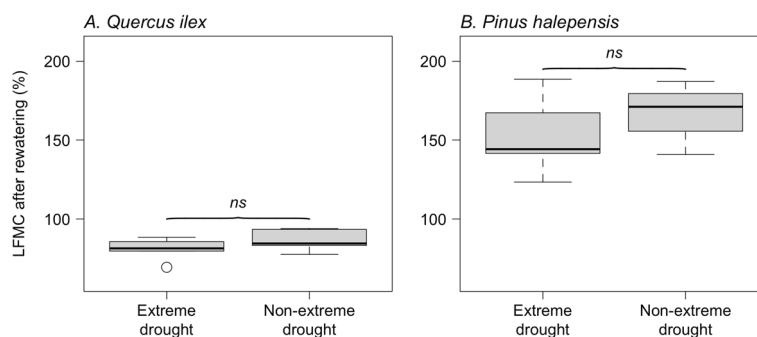Cakpo *et al. Annals of Forest Science*   (2024) 81:26

Page 8 of 16

Fig. 3 Comparison of live fuel moisture content (*LFMC*, % dry mass) of rewatered leaves previously submitted to extreme drought (minimum water potential reached by the leaves ($\Psi_{min} < -3$ MPa) and not submitted to extreme drought ($\Psi_{min} > -3$ MPa). The results are presented separately for the oak (*Quercus ilex*) and pine (*Pinus halepensis*). Significant differences were determined using *t*-tests. No significant differences are denoted as "ns"

exhibited full recovery regardless of the measurement period or drought level. Conversely, α_{Dead} and *CFMC* did not fully recover during the driest period of the experiment, with this pattern being more pronounced for oaks than for pines.

3.2 LFMC dynamics in droughted and recovery plants

We further investigated whether *LFMC* fully recovered after drought (in accordance with H1 and H3; Fig. 1) or did not fully recover due to leaf-level hydraulic dysfunction (in accordance with H2 and H4; Fig. 1). The results showed that while the average *LFMC* was lower for the leaves submitted to extreme drought for both species, our results did not show significant differences in *LFMC* values after rewatering between treatments (*t*-test; $p > 0.1$ for pine and oak) (Fig. 3).

3.3 CFMC predictions

A main goal of this study was to predict the canopy fuel moisture (*CFMC*) and identify the plant trait values that best align with empirical data. Based on previous findings (Sect. 3.2), we hypothesized that hydraulic damages at *t* leaf scale are insignificant for surviving leaves, and that extreme drought primarily impacts the rate of foliage mortality (α_{Dead}).

Our full model, based on the prediction of several fuel moisture subcomponents (*LFMC*, *DFCM*, and α_{Dead}), performed well at predicting *CFMC* for both species. For *CFMC*, the prediction metrics for pine ($R^2 = 0.87$ and $RMSE = 13.2\%$, Table 1) and oak ($R^2 = 0.87$, $RMSE = 9.4\%$, Table 2) were accurate, and no noticeable bias was observed in the predictions of our models across the range of observed values (Fig. 4A, B).

However, when looking at the predictions of the *CFMC* subcomponents, we observed disparities in model

Table 1 Fitted parameters and goodness of fit for the different submodels—live fuel moisture content (LFMC), proportion of foliage mortality in the canopy (α_{dead}), and dead fuel moisture content (DFMC)—as well as the full canopy fuel moisture content (CFMC) model for the pine species (*Pinus halepensis*). The parameters for the *CFMC* model include the osmotic potential at full turgor π_0 (MPa), the modulus of elasticity of the symplasm (ε_{Sym}, MPa), the leaf dry matter content (*LDMC*, mg.g^{-1}), and the leaf apoplasmic fraction (α_f). The parameters for the α_{dead} model are the slope (%.MPa^{-1}) and water potential for which 50% mortality is observed (ψ_{f50}, MPa). The parameter for the *DFMC* model is the rate of moisture decay with increasing VPD (*m*, %.kPa^{-1}). The performance metrics include the root-mean-square error (*RMSE*, %), the mean absolute error (*MAE*, %), and the coefficient of determination (R^2)

Model	Parameters				Performance		
LFMC	π_0	ε_{Sym}	*LDMC*	a_f	*RMSE*	*MAE*	R^2
	−2.1	22.0	381	0.35	15.3	12.8	0.84
α_{dead}	*slope*	ψ_{f50}	-	-	*RMSE*	*MAE*	R^2
	101	−6.89	-	-	6.5	5.5	0.79
DFMC	*m*	-	-	-	*RMSE*	*MAE*	R^2
	0.99	-	-	-	8.0	6.5	0.22
CFMC (full model)	-	-	-	-	*RMSE*	*MAE*	R^2
	-	-	-	-	13.2	10.8	0.87

Table 2 Fitted parameters and goodness of fit for the different submodels—live fuel moisture content (LFMC), proportion of foliage mortality in the canopy (α_{dead}), and dead fuel moisture content (DFMC)—as well as the full canopy fuel moisture content (CFMC) model for the oak species (*Quercus ilex*). The parameters for the *CFMC* model include the osmotic potential at full turgor π_0 (MPa), the modulus of elasticity of the symplasm (ε_{Sym}, MPa), the leaf dry matter content (*LDMC*, mg.g^{-1}), and the leaf apoplasmic fraction (α_f). The parameters for the α_{dead} model are the slope (%.MPa^{-1}) and water potential for which 50% mortality is observed (ψ_{f50}, MPa). The parameter for the *DFMC* model is the rate of moisture decay with increasing VPD (m, %.kPa^{-1}). The performance metrics include the root-mean-square error (*RMSE*, %), the mean absolute error (*MAE*, %), and the coefficient of determination (R^2)

Model	Parameters				Performance		
LFMC	π_0	ε_{Sym}	*LDMC*	α_f	*RMSE*	*MAE*	R^2
	-2.9	15.7	521	0.26	7.6	6.2	0.78
α_{dead}	*slope*	ψ_{f50}	-	-	*RMSE*	*MAE*	R^2
	42.5	-7.5	-	-	7.6	5.1	0.94
DFMC	m	-	-	-	*RMSE*	*MAE*	R^2
	1.06	-	-	-	6.9	38.7	0.34
CFMC (full model)	-	-	-	-	*RMSE*	*MAE*	R^2
	-	-	-	-	9.4	7.5	0.87

performance as well as differences in fitted parameters between the two species. For the LFMC model, the osmotic potential at full turgor (π_0) was higher for the pine species (-2.6 MPa) than for the oak species (-3.7 MPa). Conversely, the modulus of elasticity of the symplasm (ε_{Sym}) and leaf dry matter content (LDMC) were lower for pine (12 MPa and 369 mg.g^{-1}, respectively) than for oak (15.9 MPa and 516 mg.g^{-1}, respectively). Our results also showed that the performance of the models with α_f forced to 0 was similar or even higher than that of the original *LFMC* models. Moreover, when α_f was freely determined by the algorithm, it consistently yielded lower-than-expected values (Appendix Tables 4 and 5).

For α_{Dead}, our models also performed well for both species ($R^2 = 0.87$ and $R^2 = 0.87$ for pine and oak, respectively) (Fig. 4G, H). The fitted parameters indicated that leaf mortality occurs at a higher water potential for pine ($\psi_{f50} = -6.9$ MPa) compared to oak ($\psi_{f50} = -7.5$ MPa). For oak, ψ_{f50} is lower than the P_{50} estimated from stem vulnerability curve on mature trees (-4.6 MPa, Appendix Fig. 6 and Table 6), a species for which we also observed important differences in P_{50} for leaves and stem (Appendix Fig. 7). For pine, ψ_{f50} is similar than the P_{50} measure on mature trees (-7.6 MPa, Appendix Fig. 6 and Table 6).

Finally, the models for *DFMC* demonstrated limited predictive accuracy in both species, as indicated by low-performance metrics ($R^2 = 0.22$ and $R^2 = 0.34$ for pine and oak, respectively) (Fig. 4E, F).

4 Discussion

Our findings indicate that under severe soil water-deficit conditions, foliage mortality (increased α_{Dead}) is a significant physiological driver of canopy fuel moisture content (*CFMC*) in plant seedlings. Because foliage mortality is irreversible, the influence of leaf mortality on *CFMC* persists beyond the drought period, that is to say as long as dead leaves and twigs remain attached to the plant and new leaves are not produced (Fig. 2). This highlights the crucial role of foliage mortality in shaping the dynamics of *CFMC* during both drought and post-drought conditions and thereby supporting the hypotheses H3 and H4 of our study (Fig. 1). Consequently, our results indicated that relying solely on the current leaf water potential is insufficient for accurate *CFMC* prediction. It is crucial to consider the minimum water potential reached by the plant during the drought season (Ψ_{min}) to account for extreme drought events that may have resulted in foliage mortality. On the other hand, we did not find significant evidence of plant hydraulic damages in the surviving leaves (Fig. 3), excluding hypotheses H2 and H4 (Fig. 1). These results suggest that some leaves suffer from irreversible hydraulic damages leading to death, while the other (surviving) leaves do not seem to be affected at all and are therefore capable of recovering their initial functions.

A range of leaf and plant traits drive both the values and dynamics of *CFMC* during drought, either by shaping (i) the plant response to drought (Ψ_{Leaf}), (ii) the relationship between *LFMC* and Ψ_{Leaf}, or (iii) the response of foliage mortality to Ψ_{Leaf}. Next, we discuss the effects of plant traits on each of these processes and how physiological processes related to low water potentials differ between the two studied species. We also discuss the main limitations of our study, particularly its generalization to mature, natural forests, and suggest research pathways that could enable to investigate more deeply
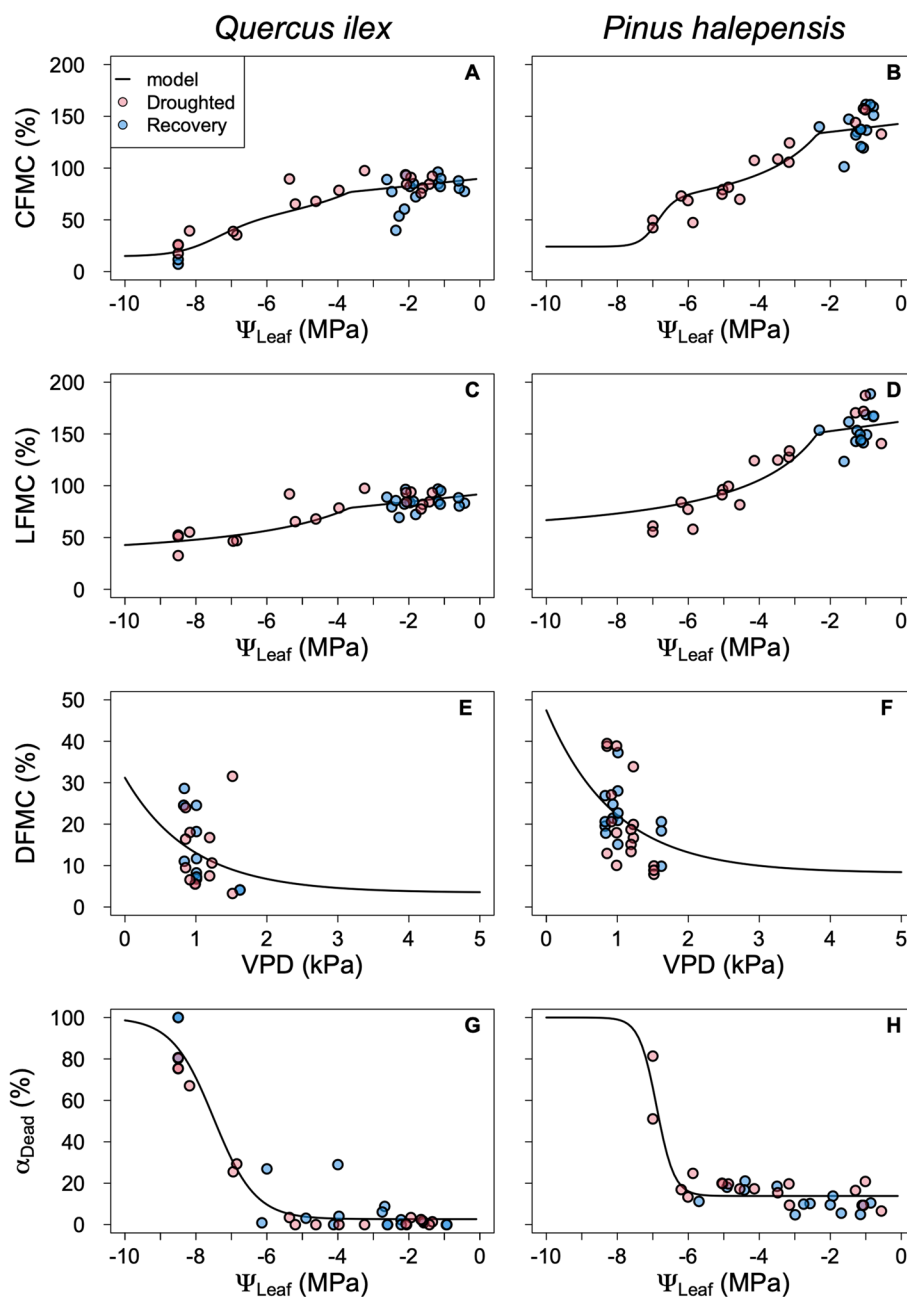
Cakpo *et al. Annals of Forest Science*   (2024) 81:26

Page 10 of 16

Fig. 4 Comparison of observed and simulated canopy fuel moisture content (*CFMC*, % dry mass), live fuel moisture content (*LFMC*, % dry mass), dead fuel moisture content (*DFMC*, % dry mass), and foliage mortality (α_{dead}, %) as a function of leaf water potential (Ψ_{Leaf}, MPa) or vapor pressure deficit (*VPD*, kPa) for pine (*Pinus halepensis*) and oak (*Quercus ilex*)

how leaf-level embolism processes impact the dynamics of fuel moisture content.

The species-dependent plant response to soil water deficit (i.e., Ψ_{Leaf} dynamics) partly explained the different fuel moisture dynamics observed between the two studied species (Fig. 2), thereby highlighting the differences in plant functional strategies previously described

by Moreno et al. (2021). Aleppo pine (*Pinus halepensis*) is generally considered a drought avoider characterized by early stomatal closure and a low resistance to drought, while Holm oak (*Quercus ilex*) is considered as a drought-tolerant tree species with a later stomatal closure but higher resistance to drought. Such differences can lead to lower transpiration rates, higher soil water content, and

Cakpo *et al. Annals of Forest Science*   (2024) 81:26

Page 11 of 16

higher Ψ_{Leaf} for Aleppo pine than for Holm oak (Fig. 2). In this study, we specifically focused on assessing the impact of soil water deficit on leaf water potential (Ψ_{Leaf}). The experimental conditions were tightly controlled, maintaining greenhouse temperatures between 25 and 35 °C and relative humidity (RH) levels between 40 and 75%. It is crucial to note that variations in vapor pressure deficit (VPD) also significantly influence Ψ_{Leaf} dynamics by controlling transpiration rates (Grossiord et al. 2020). Additionally, temperature plays a pivotal role in Ψ_{Leaf} dynamics by directly influencing cuticular conductance, which represents the primary source of water loss from plants when stomata are closed (Duursma et al. 2019).

Consistent with prior studies (Nolan et al. 2018, 2022; Scarff et al. 2021), our results confirm that the differences in *LFMC* between plant species, at a given water potential, are governed by the response of *LFMC* to Ψ_{Leaf} (*p–v* curves traits) as well as the leaf dry matter content (*LDMC*), which determines the maximum *LFMC* value (*LFMC_{sat}*). It should be noted here that the values reported for these traits in this study slightly differ from what has been measured at experimental sites in southern France. For instance, for pines, Moreno (2022) reported values of -1.5 MPa and 445 mg.mg^{-1} for π_0 and *LDMC*, respectively, which are higher than the values estimated in this study (-2.6 MPa and 369 mg.mg^{-1}). For oaks, values of -2.8 MPa and 580 mg.mg^{-1} for π_0 and *LDMC*, respectively, were reported by Moreno (2022), which are similar to the values estimated in this study (-2.9 MPa and 521 mg.mg^{-1}). These discrepancies could be due to the fact that our experiment was carried out on plant seedlings and not on mature trees. One should note, however, that the relative difference between species was coherent across studies.

Our study highlights that under extreme soil water deficits, the response of foliage mortality to declining water potential plays a major role in the dynamics of *CFMC*, aligning with the findings of Ruffault et al. (2023). In our experiment, we observed that 50% of leaf mortality in tree seedlings occurred at a water potential of -6.9 MPa and -7.5 MPa for pines and oaks, respectively. Interestingly, the difference in this threshold (0.6 MPa) between species is much smaller than their difference in stem P50, which is 2.6 MPa (considering a stem P50 of 4.8 MPa for pine and 7.4 MPa for oak, respectively). This might be explained by a greater vulnerability to embolism in leaves compared to stems in *Quercus ilex*. Indeed, leaf vulnerability curves, available only for oaks (see Appendix Fig. 7), indicate that leaves are more vulnerable to drought-induced embolism than stems. Although we lack estimates of needle P50 for Aleppo pines, previous studies have reported minimal segmentation for another pine species (*Pinus pinaster*; Bouche et al. 2016).

Exploration of key areas, such as hydraulic segmentation and phenomena like leaf persistence on the tree after death, has been so far limited. Addressing these aspects could significantly enhance our understanding of wildfires and their ecological impacts, thereby highlighting the potential for exploration through the integration of plant hydraulics into fire behavior models (Dickman et al. 2023; Torres-Ruiz et al. 2024).

Our modeling framework hypothesized that the water content of dead leaves on the tree is exclusively driven by VPD. However, our findings suggest that this assumption may not be entirely accurate (Fig. 4E, F). Indeed, the fuel moisture content of dead leaves of seedlings had higher values and a wider range of variations compared to the litter moisture content (Fig. 2E, F), which can be explained by several reasons. Firstly, recent studies have shown that lethality threshold for plant is below 100% loss of hydraulic conductivity (Hammond et al. 2019), suggesting that there might be a system of conductive tissues still supplying water to leaves until very late. Hence, leaves desiccation is more likely a progressive process, so that leaves that got partly disconnected from the vascular system within the last few days before sampling may differ in terms of water content, particularly when compared to those that got brown weeks or months ago. In addition, distinguishing between dead leaves and needles from living ones, especially for *Pinus halepensis*, posed a challenge in our experiment. It was based on a visual appreciation of leaf coloring, suggesting that some leaves or needles as could have been classified as deceased when they were not. As a result, the CFMC of canopy suffering leaf mortality could be slightly underestimated with our approach.

One notable aspect that could improve the understanding and predictions of CFMC dynamics is the consideration of the impact of leaf phenology. Leaf development and senescence influence leaf moisture dynamics by modifying the leaf dry matter content (LDMC, Eq. 4) (Jolly et al. 2014; Resco de Dios 2020; Nolan et al. 2022). In our experiment, we observed higher level of LFMC for young leaves during early stages of drought. However, young leaves LFMC values tended to reach similar levels as mature leaves during deep drought. Further study should evaluate more in depth the part of the CFMC decreases during the summer season that is related to changes in LDMC and not to the direct impact of drought water content (Jolly et al. 2014). Another mechanism that would have worth to investigate more deeply in our experiment is preprogramed needle senescence (Balaguer-Romano et al. 2020). Whereas this phenomenon is known to occur in mature pine during leaf renewal, it has not been observed on our young potted pines. However, a better understanding of this phenomenon is important

as it can modify the percent of dead needles and change the estimation of the impact of drought on foliage mortality. Further experiments or monitoring on mature tree should allow to quantify the effect of drought compared to the effect only due to the proportion of dead needles and its impact on CFMC.

More generally, the conclusions of our study are based on observations of seedlings in pots, raising questions regarding how applicable our findings are to mature trees in natural conditions. One crucial difference lies in the definition of CFMC, where our study includes leaf mortality but does not consider tree mortality, a phenomenon that could significantly impact CFMC dynamics at the ecosystem or landscape level. It is also crucial to interpret our results by recognizing disparities between experimental setups and the complexities of mature tree environments, including factors such as competition, root depth, and profile. To date, only few studies investigated the impact of drought on CFMC that includes leaf

or plant mortality (Balaguer-Romano et al. 2020; Ruffault et al. 2023); we therefore advocate for further research in this domain to enhance our understanding of CFMC dynamics in forested ecosystems.

5 Conclusion

With ongoing climate change, identifying the most vulnerable species and areas to wildfires has become a critical challenge. Our results shed light on the crucial role played by both leaf and whole-plant traits in shaping the plant response to drought in terms of fuel moisture content. Given the anticipated rise in the frequency and intensity of drought events, gaining a better understanding of the plant-hydraulic processes that contribute to drought-induced foliage mortality is crucial for assessing wildfire risks in forests and shrublands. These findings highlight the need to develop fire danger models that incorporate the mechanisms underlying plant responses to drought.
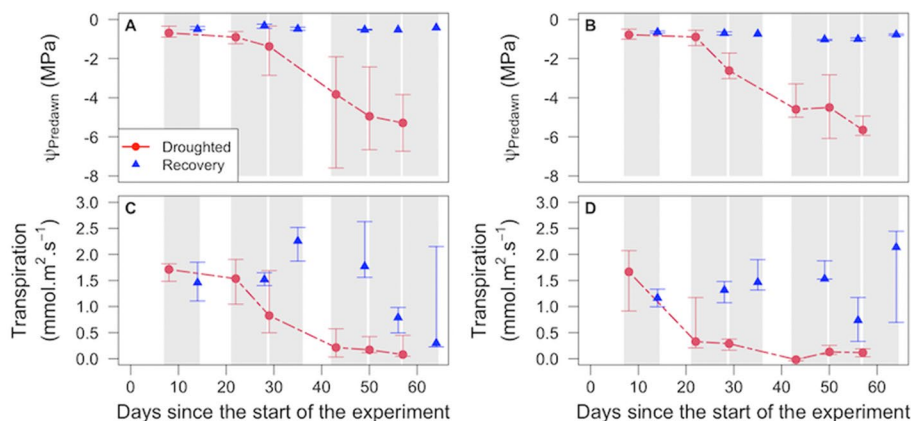
Appendix

Fig. 5 Dynamics of plant dehydration during drought and rewatering in oak (*Quercus ilex*) and pine (*Pinus halepensis*). The time dynamics of predawn water potentials ($\Psi_{predawn}$, MPa) (**A**, **B**) and plant transpiration (*mmol.m^2.s^{-1}*) (**C**, **D**) are shown. The median of measured values, along with the 5th and 95th percentiles, is shown. Red and blue circles indicate the droughted and recovery pots, respectively
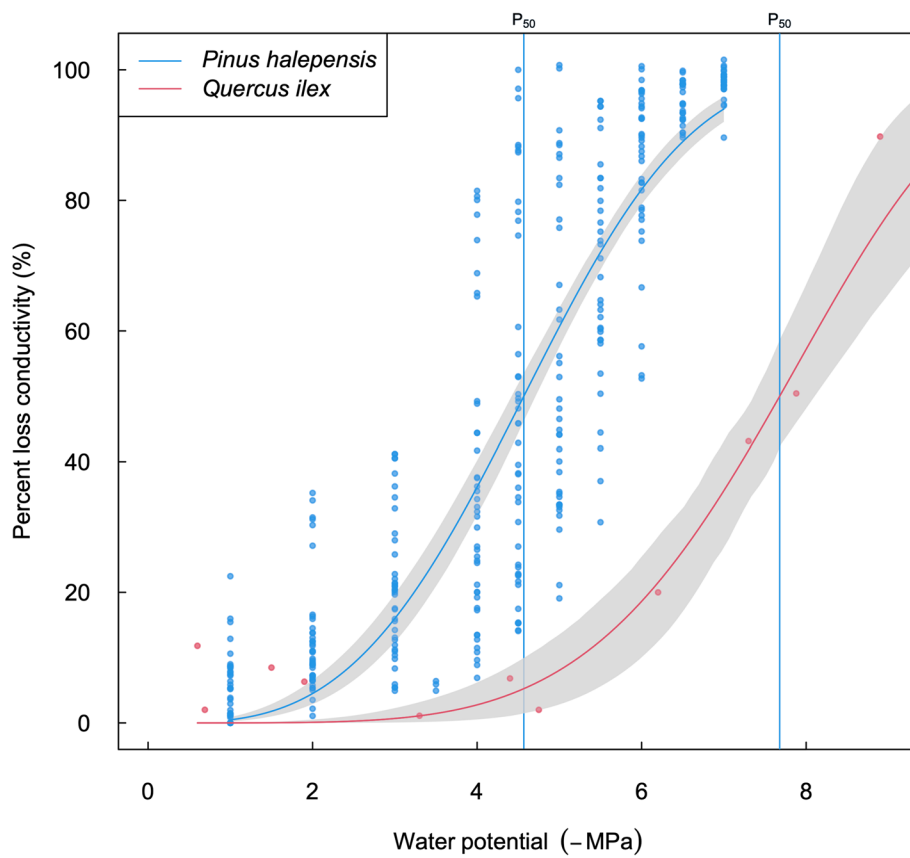
Fig. 6 Stem vulnerability curves for *Quercus ilex* and *Pinus halepensis*. For *Quercus ilex*, stem measurements were obtained from Sergent et al. (2020) conducted on 1-m-long branches sampled from 10 individual trees using Cavitron techniques (Burlett et al. 2022). Vulnerability curves for *Pinus halepensis* were extracted from Moreno (2022), and these measurements were obtained using Cavitron techniques on 15 samples collected at the Font-Blanche site in 2018
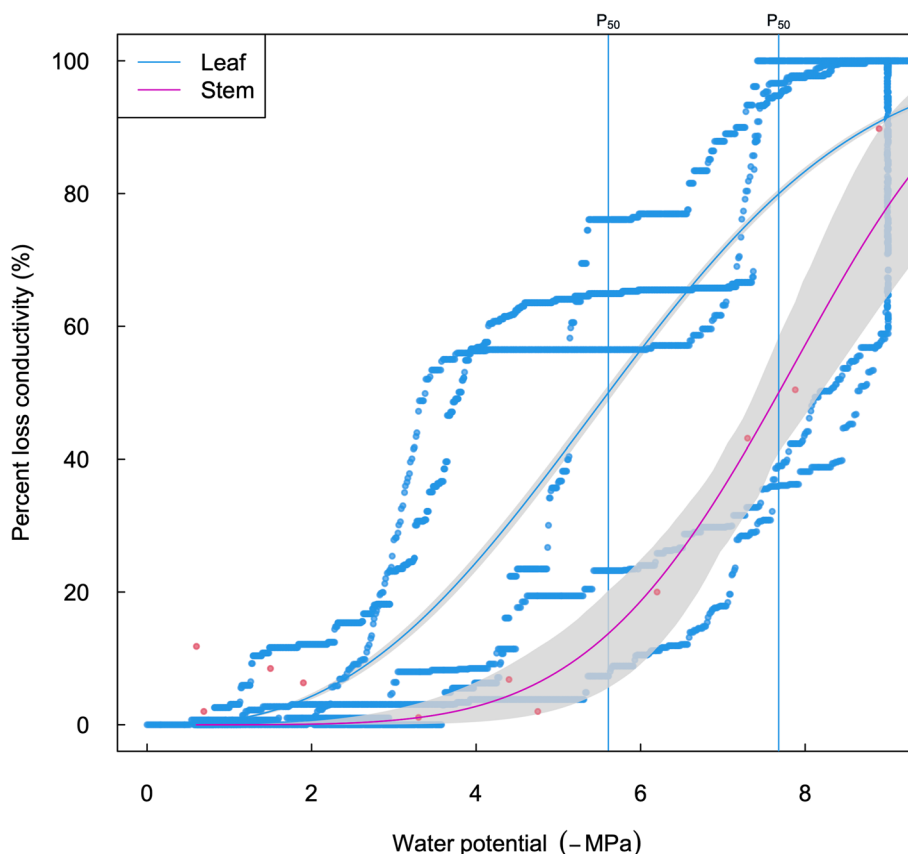
Fig. 7 Leaf and stem vulnerability curves measured for *Quercus ilex*. Stem measurements were obtained from Sergent et al. (2020), conducted on 1-m-long branches sampled from 10 individual trees using Cavitron techniques (Burlett et al. 2022). Vulnerability curves for *Quercus ilex* leaves were extracted from Moreno (2022) and derived from samples collected at the Font-Blanche site using optical techniques. The significant variability observed in leaf vulnerability curves (VC) aligns with several unpublished findings, indicating that leaf P50 values (the water potential causing 50% loss of hydraulic conductance) may exhibit greater heterogeneity compared to stem P50 values across various species (comm. pers with H. Cochard and T. Brodribb)

Table 3 Day at which each measurement campaign was carried out during the drought experiment

Measurement campaign	Number of days since the beginning of the experiment	Date
1	8	10 July 2019
2	22	24 July 2019
3	29	31 July 2019
4	43	14 August 2019
5	50	21 August 2019
6	57	28 August 2019

Table 4 Fitted parameters and goodness of fit for two alternative models for live fuel moisture content (LFMC) for the pine species (*Pinus halepensis*). The parameters for the LFMC model include the osmotic potential at full turgor π_0 (MPa), the modulus of elasticity of the symplasm (ε_{Sym}, MPa), the leaf dry matter content (*LDMC*, $mg.g^{-1}$), and the leaf apoplasmic fraction (α_f). In the first alternative model ($\alpha_f=0$), α_f was held constant at 0, completely disregarding the apoplasmic compartment. In the second model (free α_f), α_f to be determined freely by the fitting algorithm. The performance metrics include the root-mean-square error (*RMSE*, %), the mean absolute error (*MAE*, %), and the coefficient of determination (R^2)

Model	Parameters				Performance		
	π_0	ε_{Sym}	*LDMC*	α_f	*RMSE*	*MAE*	R^2
$\alpha_f = 0$	−2.6	12	369	0	13.8	11.6	0.86
Free α_f	−2.4	14.5	375	0.07	14.1	12.0	0.86

Cakpo *et al. Annals of Forest Science* (2024) 81:26

Page 15 of 16

Table 5 Fitted parameters and goodness of fit for two alternative models for live fuel moisture content (LFMC) for the oak species (*Quercus ilex*). The parameters for the LFMC model include the osmotic potential at full turgor π_0 (MPa), the modulus of elasticity of the symplasm (ε_{Sym}, MPa), the leaf dry matter content (*LDMC*, $mg.g^{-1}$), and the leaf apoplasmic fraction (α_f). In the first alternative model ($a_f=0$), a_f was held constant at 0, completely disregarding the apoplasmic compartment. In the second model (free a_f), a_f to be determined freely by the fitting algorithm. The performance metrics include the root-mean-square error (*RMSE*, %), the mean absolute error (*MAE*, %), and the coefficient of determination (R^2)

Model	Parameters				Performance		
	π_0	ε_{Sym}	*LDMC*	a_f	*RMSE*	*MAE*	R^2
$a_f = 0$	−3.7	15.9	516	0	7.8	6.5	0.76
Free a_f	−3.0	15.7	520	0.22	9.4	7.5	0.78

Table 6 Parameters of the leaf and stem vulnerability curves fitted for the two species studied: the oak (*Quercus ilex*) and the pine (*Pinus halepensis*). P_{50} is the water potential causing 50% loss of hydraulic conductance. Slope (%.MPa^{-1}) is the rate of leaf embolism spread at P_{50}

Species	Organ	Parameter	Estimate
Quercus ilex	Leaf	*Slope*	16.5 (16.1–16.9)
Quercus ilex	Leaf	P_{50}	5.6 (5.5–5.7)
Quercus ilex	Stem	*Slope*	22.2 (14.8–36.1)
Quercus ilex	Stem	P_{50}	7.7 (7.2–8.1)
Pinus halepensis	Stem	*Slope*	24.9 (22.4–27.6)
Pinus halepensis	Stem	P_{50}	4.6 (4.4–4.7)

Authors' contributions

Conceptualization, Coffi Belmys Cakpo, Julien Ruffault, Jean-Luc Dupuy, François Pimont, and Nicolas Martin-StPaul; methodology, Jean-Luc Dupuy, François Pimont, Frederic Jean, CD, and Nicolas Martin-StPaul; formal analysis, Coffi Belmys Cakpo, Nathan Jean, and Nicolas Martin-StPaul; investigation, Claude Doussan, Myriam Moreno, Nathan Jean, Frederic Jean, and Nicolas Martin-StPaul; data curation, Coffi Belmys Cakpo, Nathan Jean, and Nicolas Martin-StPaul; writing — original draft preparation, Julien Ruffault, and Nicolas Martin-StPaul; writing — review and editing, Coffi Belmys Cakpo, Julien Ruffault, Jean-Luc Dupuy, François Pimont, Claude Doussan, Myriam Moreno, Nathan Jean, Frederic Jean, Regis Burlett, Sylvain Delzon, Santiago Trueba, José M Torres-Ruiz, Hervé Cochard, and Nicolas Martin-StPaul; funding acquisition, Jean-Luc Dupuy and Nicolas Martin-StPaul; and visualization, Coffi Belmys Cakpo, Julien Ruffault, and Nicolas Martin-StPaul. The authors read and approved the final manuscript.

Availability of data and materials

The datasets used in this study are available at https://doi.org/10.57745/JTBTTF.

Declarations

Ethics approval and consent to participate
Not applicable.

Consent for publication
All authors gave their informed consent to this publication and its content.

Competing interests
The authors declare that they have no competing interests.

Reference to pre-print servers
None.

Author details
[1]INRAE, URFM, 84000 Avignon, France. [2]INRAE, Montpellier SupAgro, CIRAD, UMR AGAP Institut, Montpellier 34398, France. [3]INRAE, Avignon Université, UMR EMMAH, Avignon 84914, France. [4]INRAE, Univ. Bordeaux, BIOGECO, 33615 Pessac, France. [5]INRAE, Université Clermont-Auvergne, PIAF, 63000 Clermont-Ferrand, France. [6]Instituto de Recursos Naturales y Agrobiología (IRNAS), Consejo Superior de Investigaciones Científicas (CSIC), Seville 41012, Spain.

References

Balaguer-Romano R, Díaz-Sierra R, Madrigal J, et al (2020) Needle senescence affects fire behavior in Aleppo Pine (Pinus halepensis Mill.) stands: a simulation study. Forests 11:1054. https://doi.org/10.3390/f11101054

Bartlett MK, Scoffoni C, Sack L (2012) The determinants of leaf turgor loss point and prediction of drought tolerance of species and biomes: a global meta-analysis. Ecol Lett 15:393–405. https://doi.org/10.1111/j.1461-0248.2012.01751.x

Bouche PS, Delzon S, Choat B et al (2016) Are needles of Pinus pinaster more vulnerable to xylem embolism than branches? New insights from X-ray computed tomography. Plant Cell Environ 39:860–870

Burlett R, Parise C, Capdeville G et al (2022) Measuring xylem hydraulic vulnerability for long-vessel species: an improved methodology with the flow centrifugation technique. Ann for Sci 79:5. https://doi.org/10.1186/s13595-022-01124-0

Dickman LT, Jonko AK, Linn RR et al (2023) Integrating plant physiology into simulation of fire behavior and effects. New Phytol 238:952–970. https://doi.org/10.1111/nph.18770

Duursma RA, Blackman CJ, Lopéz R et al (2019) On the minimum leaf conductance: its role in models of plant water use, and ecological and environmental controls. New Phytol 221:693–705. https://doi.org/10.1111/nph.15395

Finney, Mark A and McAllister, Sara S and Grumstrup, Torben P and Forthofer, Jason M (2021) Wildland Fire Behaviour. CSIRO Publishing, p 377, 978-1-4863-0910-8. https://doi.org/10.1071/9781486309092, https://ebooks.publish.csiro.au/content/9781486309092/9781486309092

Gabriel E, Delgado-Dávila R, De Cáceres M et al (2021) Live fuel moisture content time series in Catalonia since 1998. Ann for Sci 78:44. https://doi.org/10.1007/s13595-021-01057-0

Grossiord C, Buckley TN, Cernusak LA et al (2020) Plant responses to rising vapor pressure deficit. New Phytol 226:1550–1566. https://doi.org/10.1111/nph.16485

Hammond WM, Yu K, Wilson LA et al (2019) Dead or dying? Quantifying the point of no return from hydraulic failure in drought-induced tree mortality. New Phytol 223:1834–1843. https://doi.org/10.1111/nph.15922

Hölttä T, Cochard H, Nikinmaa E, Mencuccini M (2009) Capacitive effect of cavitation in xylem conduits: results from a dynamic model. Plant Cell Environ 32:10–21

Johnson DM, Wortemann R, McCulloh KA et al (2016) A test of the hydraulic vulnerability segmentation hypothesis in angiosperm and conifer tree species. Tree Physiol 36:983–993. https://doi.org/10.1093/treephys/tpw031

Cakpo *et al. Annals of Forest Science* (2024) 81:26

Page 16 of 16

Jolly WM, Hadlow AM, Huguet K (2014) De-coupling seasonal changes in water content and dry matter to predict live conifer foliar moisture content. Int J Wildland Fire 23:480–489. https://doi.org/10.1071/WF13127

Jolly WM, Johnson DM (2018) Pyro-ecophysiology: shifting the paradigm of live wildland fuel research. Fire 1:8–8. https://doi.org/10.3390/fire1010008

Martin-StPaul N, Delzon S, Cochard H (2017) Plant resistance to drought depends on timely stomatal closure. Ecol Lett 20:1437–1447. https://doi.org/10.1111/ele.12851

Martin-StPaul N, Pimont F, Dupuy JL, et al (2018) Live fuel moisture content (LFMC) time series for multiple sites and species in the French Mediterranean area since 1996. Ann For Sci 75:. https://doi.org/10.1007/s13595-018-0729-3

Matthews S (2014) Dead fuel moisture research: 1991–2012. Int J Wildland Fire 23:78. https://doi.org/10.1071/WF13005

Moreno M (2022) Influence de la plasticité phénotypique et du mélange d'espèces sur la vulnérabilité hydraulique de forêts méditerranéennes. Thèse de doctorat dirigée par Davi, HendrikMartin, Nicolas et Simioni, Guillaume Sciences de l'environnement. Ecologie Aix-Marseille 2022. 2022AIXM0239, http://www.theses.fr/2022AIXM0239/document

Moreno M, Simioni G, Cailleret M et al (2021) Consistently lower sap velocity and growth over nine years of rainfall exclusion in a Mediterranean mixed pine-oak forest. Agric for Meteorol 308–309:108472–108472. https://doi.org/10.1016/j.agrformet.2021.108472

Nolan RH, Blackman CJ, de Dios VR et al (2020) Linking forest flammability and plant vulnerability to drought. Forests 11:779–779. https://doi.org/10.3390/f11070779

Nolan RH, Boer MM, Resco De Dios V et al (2016) Large-scale, dynamic transformations in fuel moisture drive wildfire activity across southeastern Australia. Geophys Res Lett 43:4229–4238. https://doi.org/10.1002/2016GL068614

Nolan RH, Foster B, Griebel A et al (2022) Drought-related leaf functional traits control spatial and temporal dynamics of live fuel moisture content. Agric for Meteorol 319:108941. https://doi.org/10.1016/j.agrformet.2022.108941

Nolan RH, Hedo J, Arteaga C et al (2018) Physiological drought responses improve predictions of live fuel moisture dynamics in a Mediterranean forest. Agric for Meteorol 263:417–427. https://doi.org/10.1016/j.agrformet.2018.09.011

Pimont F, Ruffault J, Martin-StPaul NK, Dupuy J-L (2019a) A cautionary note regarding the use of cumulative burnt areas for the determination of Fire Danger Index Breakpoints. Int J Wildland Fire 28:254–258. https://doi.org/10.1071/WF18056

Pimont F, Ruffault J, Martin-StPaul NK, Dupuy J-L (2019b) Why is the effect of live fuel moisture content on fire rate of spread underestimated in field experiments in shrublands? Int J Wildland Fire 28:127–137. https://doi.org/10.1071/WF18091

Pivovaroff AL, Emery N, Rasoul Sharifi M et al (2019) The effect of ecophysiological traits on live fuel moisture content. Fire 2:1–12. https://doi.org/10.3390/fire2020028

Pivovaroff AL, Sack L, Santiago LS (2014) Coordination of stem and leaf hydraulic conductance in Southern California shrubs: a test of the hydraulic segmentation hypothesis. New Phytol 203:842–850. https://doi.org/10.1111/nph.12850

R Core Team (2023) R: A Language and Environment for Statistical Computing. R Foundation for Statistical Computing, Vienna, https://www.R-project.org/

Rao K, Williams AP, Diffenbaugh NS et al (2022) Plant-water sensitivity regulates wildfire vulnerability. Nat Ecol Evol. https://doi.org/10.1038/s41559-021-01654-2

de Dios VR (2021) Plant-Fire Interactions: Applying Ecophysiology to Wildfire Management. Managing Forest Ecosystems. Springer International Publishing, 9783030411947. https://doi.org/10.1007/978-3-030-41192-3, https://books.google.fr/books?id=-OWkzQEACAAJ

Resco de Dios VV, Fellows AW, Nolan RH et al (2015) A semi-mechanistic model for predicting the moisture content of fine litter. Agric for Meteorol 203:64–73. https://doi.org/10.1016/j.agrformet.2015.01.002

Ruffault J, Curt T, Martin-StPaul NK et al (2018a) Extreme wildfire events are linked to global-change-type droughts in the northern Mediterranean. Nat Hazards Earth Syst Sci 18:847–856. https://doi.org/10.5194/nhess-18-847-2018

Ruffault J, Curt T, Moron V et al (2020) Increased likelihood of heat-induced large wildfires in the Mediterranean Basin. Sci Rep 10:13790. https://doi.org/10.1038/s41598-020-70069-z

Ruffault J, Limousin J, Pimont F et al (2023) Plant hydraulic modelling of leaf and canopy fuel moisture content reveals increasing vulnerability of a Mediterranean forest to wildfires under extreme drought. New Phytol 237:1256–1269. https://doi.org/10.1111/nph.18614

Ruffault J, Martin-StPaul N (2024) Ecophysiological and fuel moisture content data from an experimental drought study on *Pinus halepensis* Mill. and *Quercus ilex* L. [dataset]. V3, Recherche Data Gouv. https://doi.org/10.57745/JTBTTF. Accessed 20 June 2024

Ruffault J, Martin-StPaul N, Pimont F, Dupuy J-L (2018b) How well do meteorological drought indices predict live fuel moisture content (LFMC)? An assessment for wildfire research and operations in Mediterranean ecosystems. Agric for Meteorol 262:391–401. https://doi.org/10.1016/j.agrformet.2018.07.031

Ruthrof KX, Fontaine JB, Matusick G et al (2016) How drought-induced forest die-off alters microclimate and increases fuel loadings and fire potentials. Int J Wildland Fire 25:819–830. https://doi.org/10.1071/WF15028

Scarff FR, Lenz T, Richards AE et al (2021) Effects of plant hydraulic traits on the flammability of live fine canopy fuels. Funct Ecol 35:835–846. https://doi.org/10.1111/1365-2435.13771

Scrucca L (2013) GA}: a package for genetic algorithms in {R}. J Stat Softw 53:1–37. https://doi.org/10.18637/jss.v053.i04

Sergent AS, Varela SA, Barigah TS et al (2020) A comparison of five methods to assess embolism resistance in trees. For Ecol Manag 468:118175. https://doi.org/10.1016/j.foreco.2020.118175

Torres-Ruiz JM, Cochard H, Delzon S et al (2024) Plant hydraulics at the heart of plant, crops and ecosystem functions in the face of climate change. New Phytol 241:984–999. https://doi.org/10.1111/nph.19463

Tyree MT, Hammel HT (1972) The measurement of the turgor pressure and the water relations of plants by the pressure-bomb technique. J Exp Bot 23:267–282. https://doi.org/10.1093/jxb/23.1.267

Van Wagner CE (1987) Structure of the Canadian Forest Fire Weather Index. Can For Serv For Tech Rep 35:37

Yebra M, Dennison PE, Chuvieco E et al (2013) Remote sensing of environment a global review of remote sensing of live fuel moisture content for fire danger assessment : moving towards operational products. Remote Sens Environ 136:455–468. https://doi.org/10.1016/j.rse.2013.05.029

Publisher's Note